

# Evolution of Foam Cells in Subcutaneous Rabbit Carrageenan Granulomas

## I. Light-Microscopic and Ultrastructural Study

COLIN J. SCHWARTZ, MD, JOHN J. GHIDONI, MD,  
JIM L. KELLEY, PhD, EUGENE A. SPRAGUE, PhD,  
ANTHONY J. VALENTE, PhD, and  
C. ALAN SUENRAM, PhD

*From the Department of Pathology, The University of Texas Health Science Center, San Antonio, Texas*

With an increasing interest in the role of the monocyte-macrophage in the pathogenesis of atherosclerosis and as a progenitor of plaque intimal foam cells, a model for the study of foam-cell differentiation in an extravascular environment has been developed. Granulomas were induced in 25 normocholesterolemic (NC) and 28 hypercholesterolemic (HC) rabbits by the subcutaneous injection of 15 ml of 1% carrageenan. Granuloma tissue was harvested at 4, 7, 14, and 28 days and studied by light and transmission electron microscopy. Macrophages and foam cells were isolated by enzymic dispersion with collagenase and cultured for further characterization by scanning electron microscopy, nonspecific esterase (NSE),

and oil red O (ORO) staining. Granuloma macrophages from NC rabbits were consistently ORO-negative, contrasting with those from HC rabbits which were strongly ORO-positive, even at 4 and 7 days. With an increasing duration of exposure to hypercholesterolemia, macrophages accumulated increasing amounts of stainable lipid, and in the 28-day HC granulomas, large foam cells distended by lipid inclusions accounted for 70% of the cells present. This model has established that NSE-positive macrophages in HC granulomas accumulate lipid and assume the morphologic characteristics of atheromatous intimal foam cells. (*Am J Pathol* 1985, 118:134-150)

THERE IS an increasing body of evidence indicating that the pathogenesis of atherosclerosis has one or more inflammatory components. Advanced lesions in man are characterized by a prominent lymphocytic infiltrate, predominantly adventitial,<sup>1</sup> and frequent granulomatous foci.<sup>2,3</sup> In experimental hypercholesterolemia and during atherogenesis, monocyte-macrophage recruitment to the arterial intima is enhanced in a variety of species, including rabbits,<sup>4-6</sup> rats,<sup>7,8</sup> pigs,<sup>9-11</sup> birds,<sup>12</sup> and various nonhuman primates.<sup>6,13-15</sup> Tissue macrophages of peripheral blood monocyte origin<sup>16</sup> play an important role in inflammation, serving as scavengers or secretory cells<sup>17,18</sup> and as regulators of lymphocyte function.<sup>19,20</sup> In the arterial intima their putative role as progenitors of at least part of the plaque foam-cell population has been demonstrated in both rabbits and nonhuman primates on the basis of a number of features, including the presence of Fc and C<sub>3</sub> receptors, acid lipase activity, and lysozymelike antigen.<sup>6</sup> For a better understanding of the role(s) of the monocyte-macrophage in atherogenesis, it appears important that the evolving foam cell be characterized during its

differentiation with respect to surface receptor identity markers, the activation status as measured by lysosomal enzyme release and superoxide anion generation, lipoprotein uptake and catabolism, lipid composition and metabolism, and lipoprotein lipase secretion and release. Toward these objectives we have developed a model for the production of foam cells in the extravascular environment by the induction of subcutaneous carrageenan granulomas in animals rendered hypercholesterolemic by dietary cholesterol-oil supplementation.<sup>21</sup> We undertook this component of our studies to characterize the light-microscopic and ultrastructural features of granuloma foam cells during their differen-

Supported by NHLBI Grants 1-PO1-HL26890 and HL-07446.

Accepted for publication August 23, 1984.

Address reprint requests to Dr. Colin J. Schwartz, Department of Pathology, The University of Texas Health Science Center, 7703 Floyd Curl Dr., San Antonio, TX 78284.

tiation and to define the conditions for their isolation and culture.

## Materials and Methods

### Animals

Male adult New Zealand White rabbits ranging in initial weight from 2.2 to 4.0 kg were used.

### Granuloma Induction

The rabbits were anesthetized with a combination of 25 mg of ketamine (Ketalar, Parke-Davis, Morris Plains, NJ) and 5 mg of xylazine (Rompun, Bayvet Division, Cutter Laboratories, Shawnee, Kans) per kg body weight. The anterior abdominal wall was shaved and the skin sterilized with a combination of 70% ethanol and Prepodyne Solution (American Sterilizer Co., Erie, Pa). Fifteen milliliters of a sterile 1% (wt/vol) solution of carrageenan (Gelcarin HMR, Marine Colloids Division, FMC Corporation, Rockland, Maine) in physiologic saline (0.85%, wt/vol) at 37 C was slowly injected subcutaneously in the midline of the anterior abdominal wall.

### Experimental Design

Figure 1 shows the design of the study. Carrageenan granulomas were induced in 25 normocholesterolemic (NC) rabbits fed *ad libitum* with rabbit pellets (Wayne Feed Division, Continental Grain Co., Chicago, Ill), and in 28 hypercholesterolemic (HC) rabbits fed a diet supplemented with cholesterol-peanut oil blended in the following proportions: pellets, 75g; cholesterol (USP grade), 0.25 g; and peanut oil, 6.0 ml. The cholesterol was dissolved in warmed oil prior to blending. The cholesterol-oil diet was started 28 days prior to carrageenan injection and was continued until sacrifice. At 4, 7, 14, and 28 days the rabbits were exsanguinated, and the granulomas were harvested. Serum total cholesterol was determined at sacrifice with the use of an automated enzymatic procedure.<sup>22</sup> Representative samples of granuloma tissue were used for morphologic assessment, and the remainder were used for macrophage culture.

### Morphology

Granuloma tissue samples (2–4 mm) were studied by light microscopy with the use of a combination of tease preparations, paraffin and frozen sections, and 1- $\mu$  Araldite-embedded thick sections. Both the tease preparations and frozen sections were stained with oil red O (ORO) for neutral lipid. Nonspecific esterase stain-

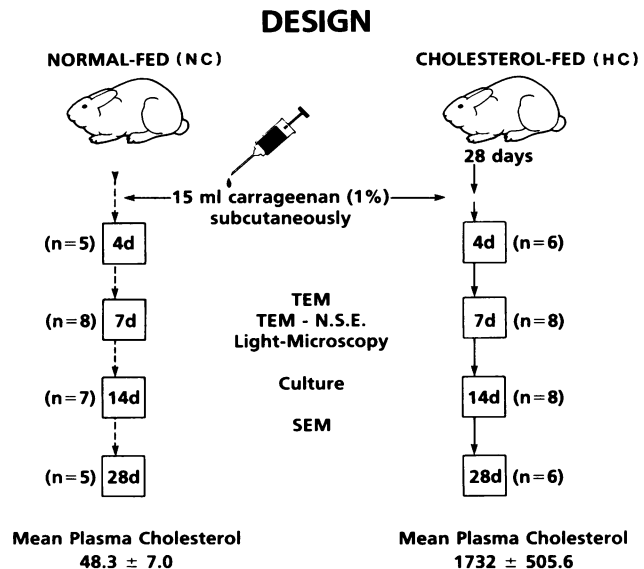


Figure 1 — Schematic of experimental design, with numbers of animals in each time and diet group in parentheses.

ing (NSE), used as a putative marker of monocytes and monocyte-derived macrophages, employed  $\alpha$ -naphthyl acetate as substrate<sup>23,24</sup> and methyl green as a counterstain. Control preparations were incubated in the absence of substrate or in the presence of NaF (1.5 mg/ml). Paraffin sections were cut at several levels and stained with hematoxylin and eosin (H&E).

For transmission electron microscopy, tissue samples were diced to approximately 1 cu mm and fixed in a combination of 2.5% glutaraldehyde and 2% paraformaldehyde in 0.1 M Na cacodylate buffer. The tissue was postfixed in aqueous buffered 1% OsO<sub>4</sub> for 1 hour, dehydrated, and embedded in Araldite 502. Ultrathin sections were stained with 2% aqueous uranyl acetate and Reynold's lead citrate for examination in either a Philips 301 or a JEOL 100 CX electron microscope.

Nonspecific esterase activity at the ultrastructural level employed a procedure using 2-naphthyl thiol acetate (NTA) as substrate.<sup>25</sup> After an initial fixation in 2.5% glutaraldehyde and 2% paraformaldehyde in 0.1 M Na cacodylate for 4 hours at 4 C, the tissue dices were incubated in buffered NTA substrate (pH 7.4) containing Fast Blue BB Salt (Sigma, St. Louis, Mo) as the coupling agent for 6 hours, washed twice with 0.1 M Na cacodylate buffer, and postfixed in 1% aqueous OsO<sub>4</sub> for 6 hours. Control preparations were processed similarly, but with the substrate (NTA) absent.

### Granuloma Macrophage Culture

Granuloma tissue dissected from the anterior abdominal wall was finely minced with scissors in sterile

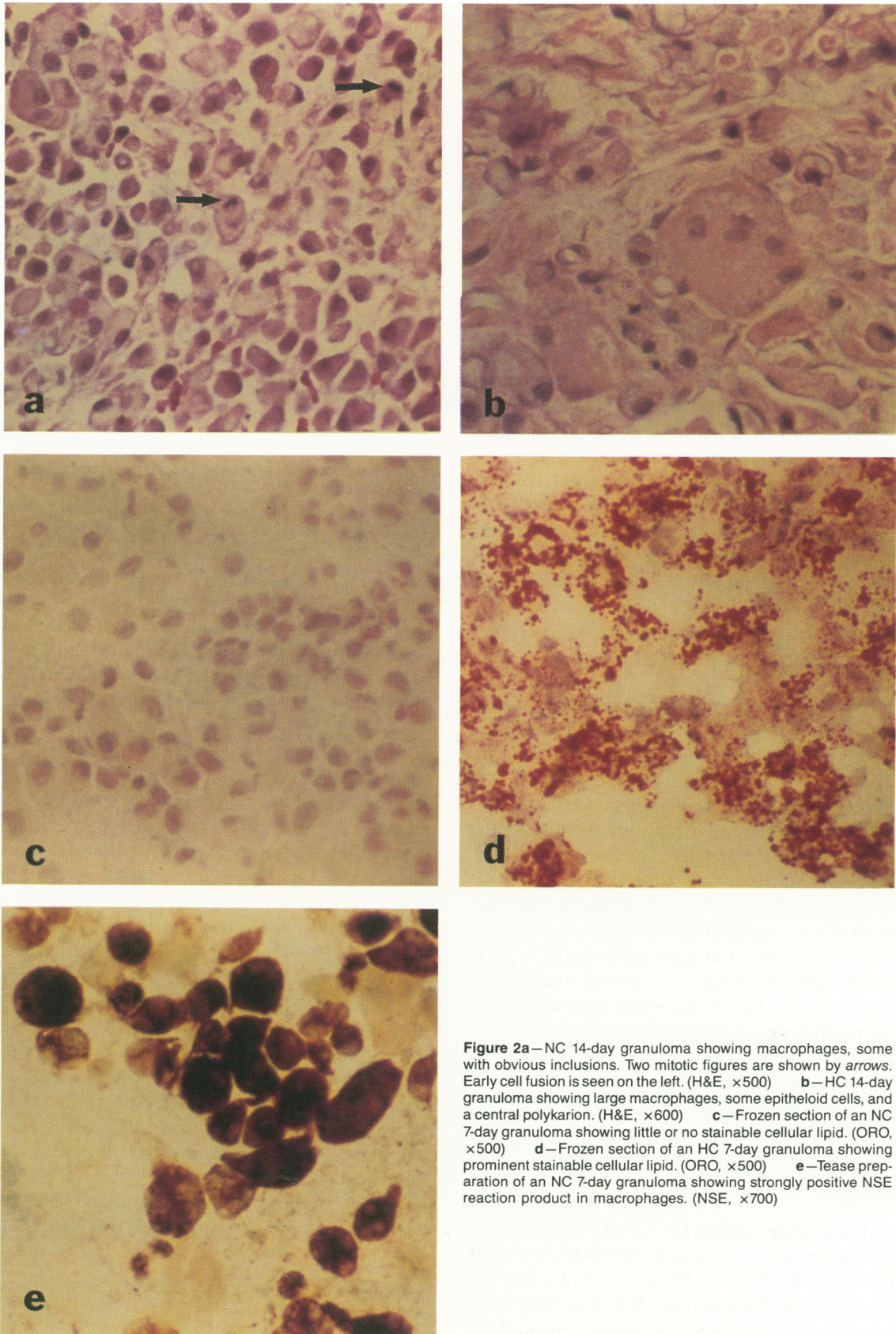


**Figure 2a**—NC 14-day granuloma showing macrophages, some with obvious inclusions. Two mitotic figures are shown by *arrows*. Early cell fusion is seen on the left. (H&E,  $\times 500$ ) **b**—HC 14-day granuloma showing large macrophages, some epitheloid cells, and a central polykaryon. (H&E,  $\times 600$ ) **c**—Frozen section of an NC 7-day granuloma showing little or no stainable cellular lipid. (ORO,  $\times 500$ ) **d**—Frozen section of an HC 7-day granuloma showing prominent stainable cellular lipid. (ORO,  $\times 500$ ) **e**—Tease preparation of an NC 7-day granuloma showing strongly positive NSE reaction product in macrophages. (NSE,  $\times 700$ )



Petri dishes in a laminar flow hood. The minced tissue was agitated in a shaking water bath for 1 hour at 37 C in 25 ml of a sterile filtered incubation medium containing collagenase (Type I, Worthington), 1 mg/ml, and soybean trypsin inhibitor (Sigma, St. Louis, Mo), 0.25 mg/ml, prepared in Dulbecco's phosphate-buffered saline (PBS), pH 7.4, with  $\text{Ca}^{2+}$  and  $\text{Mg}^{2+}$  present. The resulting turbid fluid with residual tissue fragments was then gently teased through a sterile nylon mesh filter (catalog no. HC3-183, TETKO Inc., Elmsford, NY), and the cell-rich filtrate was collected in graduated 50-ml polypropylene centrifuge tubes. Filtration of the viscous digestate was assisted by the periodic addition of M199 (GIBCO, Grand Island, NY) containing 20% fetal calf serum (FCS) to the gellike mass on the filter. The tubes were made up to a volume of 50 ml with M199 containing 20% FCS. Duplicate viable cell counts were determined with the use of a hemocytometer, and the cells were centrifuged at 1000g for 10 minutes at 14 C. Cell pellets were resuspended in M199 plus 20% FCS to a concentration of  $2 \times 10^6$ /ml and plated at densities of  $2.5\text{--}5.0 \times 10^5$ /sq cm in 35-mm glass Petri dishes, some containing glass coverslips. The medium was removed after 2 hours, the cells were rinsed, and 2 ml M199 containing 20% FCS was added to maintain culture.

The cultured cells were examined by light microscopy, under phase, and after NSE and H&E staining, and by scanning electron microscopy, with the use of preparative techniques already described in detail.<sup>26</sup>

## Results

### Gross Appearance of Granulomas

Excised granuloma tissue ranged in weight from 7 to 14 g, with color and consistency varying with the nature of the diet (NC or HC) and granuloma age. At 4 days the NC and HC granulomas were indistinguishable, each exhibiting a gelatinous or myxoid consistency and a gray somewhat translucent appearance with hemorrhagic mottling. With increasing age both the NC and HC granulomas became less myxoid, and at 14 and 28 days the tissue was clearly firmer, paler, and more fibrotic. HC granulomas at 14 and 28 days differed from their NC pairs in exhibiting a pale yellow to orange mottling. Vascularization became grossly recognizable at 7 days.

### Light Microscopy—NC Granulomas

In H&E-stained paraffin sections, NC granulomas showed a series of changes with increasing age. At 4

days, the principal histologic features were those of an acute inflammatory response. A modest polymorphonuclear leukocytic infiltrate was observed, together with slight focal interstitial hemorrhage and a diffuse sprinkling of both mononuclear cells and macrophages within the loose, slightly vascular stroma containing floccular carrageenan. Some elongate cells resembling fibroblasts and a few lymphocytes and plasma cells were also seen. Seven-day granulomas exhibited abundant large macrophages containing reticular or vacuolated inclusions. These appeared either in confluent sheets or perivascular nodules, sometimes infiltrating the muscle of the anterior abdominal wall. Vascularization of the 7-day lesions was prominent. Straplike elongate cells, similar to those of the 4-day lesions, were present, together with some loose collagen, and occasional granulocytes, lymphocytes, and monocytes. Occasional mitotic figures in cells resembling macrophages were observed, with a frequency of up to two per high-power field.

By 14 days the granulomas were distinctly more fibrous, and macrophages containing inclusions of variable size were prominent (Figure 2a), with some tendency to form nodular arrays. Large epithelioid cells, in various stages of fusion, and multinucleate cells were seen (Figure 2b). Elongate cells, resembling fibroblasts, were frequent. Monocytes were inconspicuous, but an occasional granulocyte was observed. The transition from 14- to 28-day lesions was characterized by an increasing amount of dense fibrous tissue. Macrophages remained prominent, and epithelioid and multinucleate giant cells were frequent. Monocytes were inconspicuous, and granulocytes were not seen. From 7 through 28 days the macrophages of the NC granulomas showed no discernible increase in size.

Lipid staining with ORO of both frozen sections and tease preparations of intact cells revealed that the NC granuloma macrophages at all ages were essentially free of stainable neutral lipid (Figure 2c), with only an occasional cluster of cells showing the presence of very fine cytoplasmic droplets. With NSE staining of both tease preparations and frozen sections, cells with the morphologic appearance of either monocytes or macrophages were strongly NSE-positive, with prominent red-brown cytoplasmic granules (Figure 2e). Other cells, including lymphocytes and elongate fibroblastlike cells, were either NSE negative or only faintly positive. At 7 days greater than 80% of the cells were strongly positive, but with increasing age and the presence of more fibroblastlike cells at 14 and 28 days, this declined proportionately. The NSE reaction was consistently negative in the absence of substrate. However, in the presence of substrate and NaF, some cells, including macrophages, remained moderately NSE-positive.

Table 1—The Cellular Distribution in Evolving Granulomas Expressed as a Percentage of the Total Cells Identified Ultrastructurally Within Each Diet Group and Time Period\*

Morphologic cell type	Diet group	Age of carrageenan granuloma			
		4 days	7 days	14 days	28 days
Monocytes	NC	9.3	2.2	—	1.8
	HC	7.1	2.1	3.8	1.0
Macrophages	NC	86.0	79.6	93.2	89.1
	HC	90.5	84.5	82.5	29.8
Foam cells	NC	—	—	—	—
	HC	—	13.4	11.7	69.2
Granulocytes	NC	—	13.6	4.6	1.8
	HC	2.4	—	1.0	—
Lymphocytes	NC	1.6	4.6	2.2	7.3
	HC	—	—	1.0	—
Plasma cells	NC	3.1	—	—	—
	HC	—	—	—	—
Number of cells identified	NC	64	44	88	55
	HC	42	142	103	117

\* Fibroblasts and vascular smooth-muscle cells were excluded from these calculations. The fibroblast data are presented separately in Figure 9. Monocytes were differentiated from macrophages on the basis of several criteria, the latter being larger and exhibiting prominent lysosomal inclusions, numerous cytoplasmic projections, and peripheral condensation of nuclear heterochromatin.

### Light Microscopy—HC Granulomas

With H&E-stained paraffin sections, granuloma tissue from HC rabbits showed many similarities to that from NC animals, but with some notable differences. At 4 days, while the overall cellular composition of the lesions appeared similar, the macrophages were more prominent and in particular were larger, with a vesicular cytoplasm, reflecting both the ingested carrageenan and cytoplasmic lipid inclusions. Morphologically, however, no foam cells were seen at this time. By 7 days, the HC granulomas exhibited both sheets and nodular arrays of large macrophages, some of which were distended by clear vacuolar lipid inclusions and could be recognized as foam cells. The macrophages were clearly larger than those seen in the NC lesions at 7 days, a difference which persisted through 14 and 28 days. Multinucleate giant cells made their appearance at 7 days and were seen with increasing frequency thereafter (Figure 2b).

Although the cellular composition of the 14-day NC and HC granulomas remained essentially similar, macrophages distended by numerous large and small lipid inclusions morphologically resembling foam cells were prominent in the HC lesions. Typical epithelioid cells,

some in the process of fusion, together with multinucleate cells, were frequent, as in the NC lesions.

At 28 days the more fibrotic HC granulomas were characterized by many large foam cells, distended by both large and small lipid inclusions.

NSE-staining of both tease preparations and frozen sections of HC granulomas revealed that monocytes, lipid-rich macrophages, and typical foam cells were strongly NSE-positive, indicating that the massive accumulation of lipid in the granuloma macrophages does not suppress their NSE-staining capacity. As with NC macrophages, the NSE reaction was completely inhibited in the absence of substrate, but only partially by NaF.

In contrast to the virtual absence of appreciable ORO-stainable lipid in NC granuloma macrophages, the macrophages from HC granulomas revealed considerable ORO-positive lipid in both large and small cytoplasmic droplets as early as 4 days. Increasing lipid accumulation occurred thereafter, with considerable distension of the macrophage-derived foam cells by large numbers of ORO-positive cytoplasmic droplets at 7, 14, and 28 days (Figure 2d).

In two animals, loculated bacterial abscesses were found, and these were excluded from further morphologic or culture studies.

### Ultrastructure of NC and HC Granulomas

Within the limitations of differing tissue sample size, there was good overall agreement between the observations made at the light- and electron-microscopic levels.

### Four-Day Lesions

At 4 days, the salient fine-structural features of NC granulomas were those of loose vascular granulation tissue. Extracellular residual carrageenan persisted as a floccular to finely granular material of intermediate electron density. Of the cells enumerated, 9.3% had the morphologic appearance of monocytes, and 86.0% were identified as macrophages (Table 1). The macrophages exhibited the customary peripheral cytoplasmic projections, some peripheral condensation of nuclear heterochromatin, and copious large and small membrane-bound inclusions, mostly containing a floccular material resembling ingested carrageenan. Myelin bodies were inconspicuous or absent, and the inclusions, presumably lysosomal, showed no tendency to fusion,

with their limiting membranes essentially intact. Also identified in the 4 day NC lesions were elongate fibroblasts with a prominent moderately dilated rough endoplasmic reticulum (RER) and occasional lymphocytes and plasma cells. Granulocytes (or pseudo-eosinophils) were inconspicuous. Occasional smooth-muscle cells, associated with neovascularization, were seen. Extracellular fibrin was not identified.

The overall cellular composition of the 4-day HC granulomas was similar to that of NC granulomas (Table 1): 7.1% of the HC lesions cells were identifiable as monocytes, 90.5% were identified as macrophages, and no foam cells were present. Macrophages of the HC lesions exhibited a number of fine-structural differences. Although large and small carrageenan-containing inclusions were again prominent, some were not membrane-bound, and others showed an incomplete membrane structure, with a tendency to coalescence or fusion. Additionally, many of the HC macrophages exhibited multiple small electron-translucent membrane-bound inclusions not seen in the NC macrophages, an appearance consistent with lysosomal lipid accumulation. Further, the HC macrophages contained numerous laminated myelin forms, both within membrane-bound inclusions and also free within the cytoplasm, a finding which contrasts sharply with their paucity in NC macrophages. Thus, as early as 4 days, macrophages of the NC and HC granulomas exhibit a number of consistent fine structural differences.

### Seven-Day Lesions

The 7-day NC granulomas were relatively similar in cellular composition and appearance to the 4-day lesions: 2.2% of the cells were identified as monocytes, and 79.6% were identified as macrophages (Table 1). Small and large mainly membrane-bound carrageenan-containing inclusions persisted (Figure 3a), some showing coalescence. Occasional myelin forms were seen, but these were relatively inconspicuous. Fibroblasts, appearing as elongate cells with a prominent dilated RER, were two times more frequent at 7 days, and small numbers of granulocytes and lymphocytes were identified. Some necrotic cells of indeterminate origin were seen in the NC granulomas for the first time.

In 7-day HC granulomas, 2.1% of the cells were monocytes, 84.5% macrophages, and 13.4% had the distinctive appearance of foam cells, the latter exhibiting a cytoplasm containing small electron-translucent inclusions, both membrane-bound and non-membrane-

bound, some showing fusion. The macrophages showed persistent large and small carrageenan-containing inclusions (Figure 3b), the floccular material exhibiting a somewhat more reticular pattern with intervening electron-translucent areas. The limiting membranes of these inclusions were frequently incomplete, and coalescence or fusion was common. Both the macrophages and foam cells contained myelin bodies, both within lysosomal inclusions and apparently free within the cytoplasm.

Most of the macrophages also contained variable numbers of small clear inclusions similar in size and electron translucency to those characteristic of aortic foam cells (Figure 3b). These clearly provided evidence of a continuous morphologic transition from the typical monocyte-derived macrophage, on the one hand, to the distinctive distended foam cell, on the other.

### Fourteen-Day Lesions

At 14 days the NC granulomas contained neither monocytes nor foam cells. Ninety-three percent of the cells were macrophages with predominantly large, mostly membrane-bound inclusions containing floccular ingested carrageenan, some with a reticular pattern. Inclusions frequently showed various phases of coalescence or fusion (Figure 4a). Myelin bodies, while present, were inconspicuous. Fibroblasts with a prominent RER, often in close apposition to macrophages, were most numerous at 14 days, and a moderate amount of collagen was apparent. Only an occasional lymphocyte or granulocyte was seen.

The cellular composition of the 14-day HC granulomas was similar to that of 7-day HC lesions, with 3.8% of the cells identified as monocytes, 82.5% as macrophages, and 11.7% as distinct foam cells, with their cytoplasm distended by large numbers of clear, small inclusions (Table 1). The macrophages, larger than their 14-day NC counterparts, exhibited prominent lysosomal and cytoplasmic myelin, large and smaller carrageenan-containing inclusions with frequent coalescence, and small, clear inclusions, which, with increasing numbers, presented a spectrum of transitions to the fully developed foam cell (Figure 4b). Other cells observed in the HC lesions included fibroblasts, although not as prominent as in the 14-day NC granulomas, and an occasional granulocyte and lymphocyte. Some smooth-muscle cells, associated with new vessels, exhibited occasional clusters of small, clear inclusions similar to those of the foam cells. Polykarion formation was also

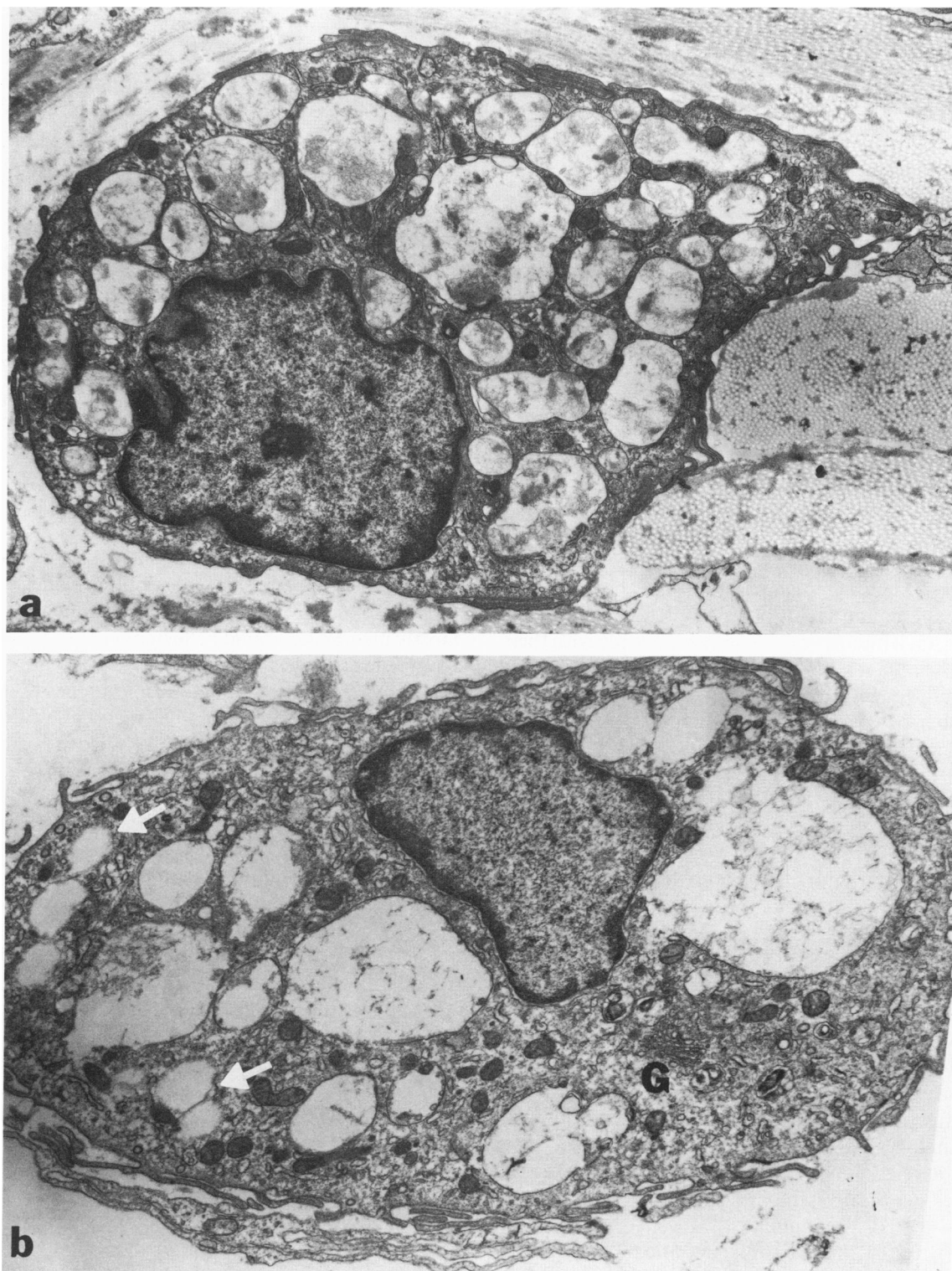


**Figure 3a**—A 7-day NC macrophage with multiple lysosomal carrageenan inclusions. Peripheral condensation of nuclear heterochromatin can be seen. ( $\times 9700$ ) **b**—A 7-day HC macrophage with large lysosomal carrageenan inclusions and some smaller electron-translucent inclusions (arrows). Cytoplasmic processes are prominent. The Golgi apparatus (G) is readily identifiable. ( $\times 12,000$ )

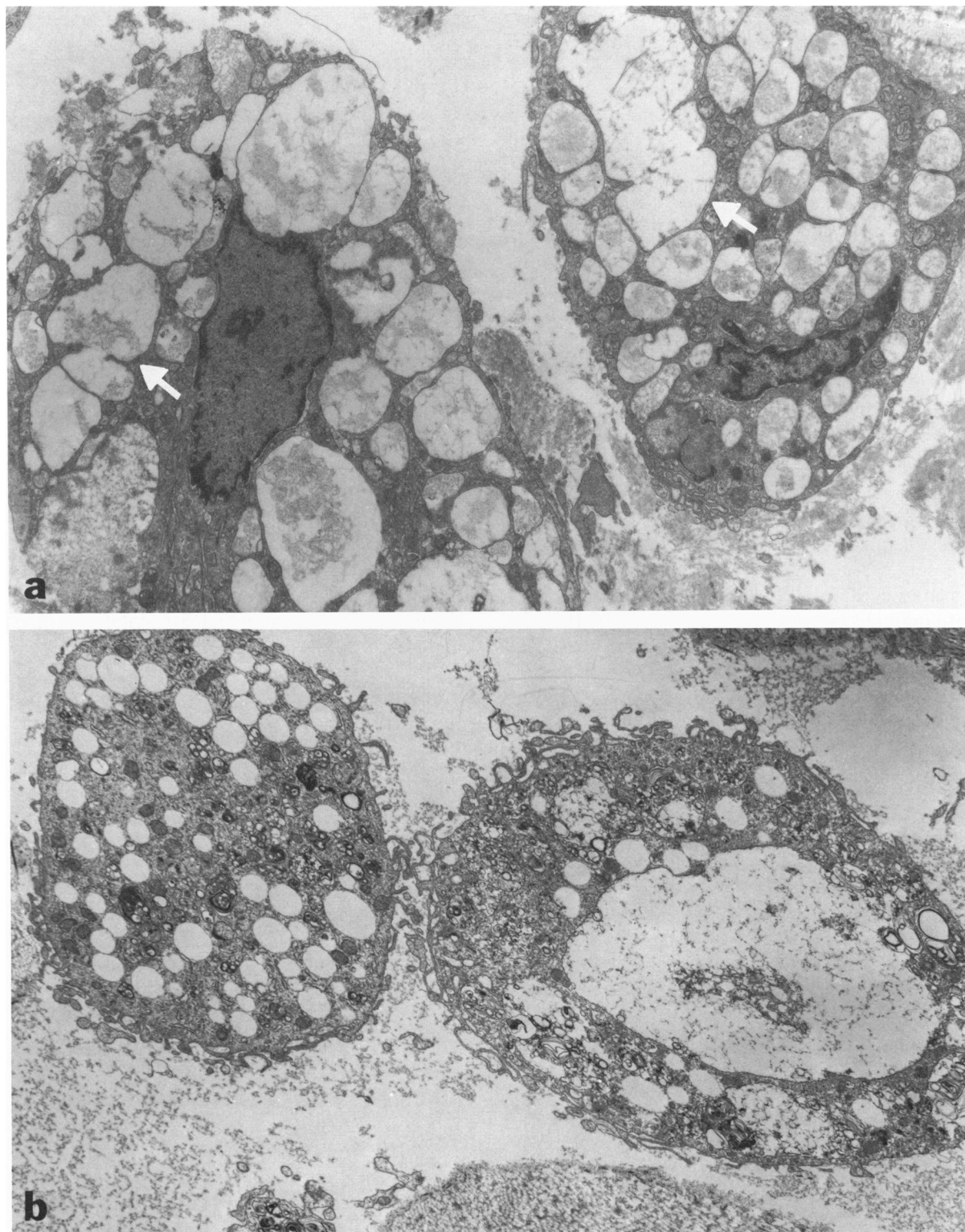


**Figure 4a** – NC 14-day macrophages with large and small lysosomal carrageenan inclusions, some of which appear to exhibit fusion (*arrows*). Myelin forms are inconspicuous. ( $\times 5800$ )    **b** – HC 14-day macrophages with large and small inclusions, prominent myelin forms, and numerous small electron-translucent inclusions, some of which have no limiting membranes. ( $\times 5800$ )



observed. Collagen was clearly more abundant than in the 7-day lesions.

### Twenty-Eight-Day Lesions

In the 28-day NC granulomas, monocytes were sparse (1.8%), and macrophages were (89.1%) the dominant cell. The occasional granulocyte and lymphocyte were observed, and fibroblasts with a prominent dilated RER were frequent, tending to be closely applied or almost wrapped around the macrophages. Collagen was prominent. Epithelioid cell fusion resulted in frequent polykaryons, with complex multilamellar interdigitating membranous nexi. Macrophage inclusions were of varying size, some showing coalescence and most containing floccular carrageenan (Figures 5 and 6). Myelin bodies, while present, were not prominent.

The 28-day HC granulomata differed markedly from the 28-day NC lesions, in that well-developed foam cells comprised 69.2% of the cell population (Figures 5b, 7, 8c), while macrophages comprised 29.8% and monocytes (1%) were sparse. As in earlier HC lesions, macrophages in various stages of transition to foam cells were present, with cells showing both large and small carrageenan containing inclusions and variable numbers of small electron translucent inclusions (Figures 5b, 7, 8c). Coalescence of small inclusions was noted (Figures 7, 8c). Collagen was also prominent in the HC lesions. Cell necrosis and interstitial cellular debris were seen. Fibroblasts, while present, were less numerous than in the NC lesions (Figure 9).

### Ultrastructural Nonspecific Esterase (NSE) Activity in Granuloma Macrophages

As described earlier, NSE activity was examined ultrastructurally with 2-naphthyl thiol acetate (NTA) as substrate on 14-day and 28-day NC and HC granuloma macrophages and foam cells. Carrageenan-containing macrophages of 14-day and 28-day NC granulomas exhibited NSE reaction product, appearing as round or ovoid electron-dense bodies of variable size (Figure 8a). While many were topographically associated with membrane-bound lysosomal inclusions, others showed no such association, appearing free within the cytoplasm (Figure 8a). NSE-positivity was retained in the macrophages and foam cells of the 14-day and 28-day HC granulomas (Figure 8b). In the foam cells the electron-dense bodies were present both within many of the numerous electron-translucent inclusions and also within some of the membrane-bound granular inclusions (Figure 8b). As in the NC macrophages, some, however, also appeared free within the cytoplasm.

No clear difference in the distribution or amount of NSE reaction product in NC macrophages and HC macrophages or foam cells was discerned. Small amounts of reaction product were noted in some neovascular smooth-muscle cells.

### Macrophage Cultures

These studies have established the feasibility of enzymatic dispersion and isolation of macrophages for culture from both NC and HC granulomas. As their characterization ultrastructurally, enzymatically, immunologically, and biochemically will be reported separately,<sup>27</sup> we describe here some selected observations on the cells from 14-day granulomas only. Cell yields ranged from  $8.2$  to  $13.6 \times 10^6$  per granuloma with no consistent difference between NC and HC lesions. Adherent cells in the culture were predominantly NSE-positive (>90%), with occasional straplike cells and other cells of uncertain identity showing little or no reaction product. The NSE-staining was largely abolished by NaF and completely with substrate absent. With scanning electron microscopy the macrophages cultured from HC granulomas were consistently larger than their NC counterparts, some showing multiple small ovoid bulges or protrusions, which are tentatively interpreted as representing cellular lipid inclusions.

Adherent macrophages from both NC and HC granulomas showed considerable morphologic variation with scanning electron microscopy, some polyhedral or more rounded cells showing extensive aprons of attachment and spreading (Figure 10), while others were more elongate. Long, attenuated cytoplasmic projections were frequent.

### Discussion

Carrageenan, a long-chain sulfated polysaccharide derived principally from Irish sea moss, *Chondrus crispus*, has been fractionated into two discrete components, namely kappa- and lambda-carrageenans with potassium chloride.<sup>28</sup> Kappa-carrageenan, which comprises some 40% of the carrageenan extract,<sup>29</sup> is composed of sulfated D-galactose and 3,6-anhydro-D-galactose in equimolar ratios and has a branched structure.<sup>30,31</sup> Lambda-carrageenan is composed principally of sulfated D-galactose<sup>32</sup> and appears to be more active than the kappa-fraction in eliciting either acute<sup>33</sup> or chronic inflammation.<sup>34</sup> The carrageenan used in the present study consisted of both kappa and lambda moieties.

Since the initial observation of Robertson and Schwartz<sup>35</sup> that subcutaneously injected carrageenan

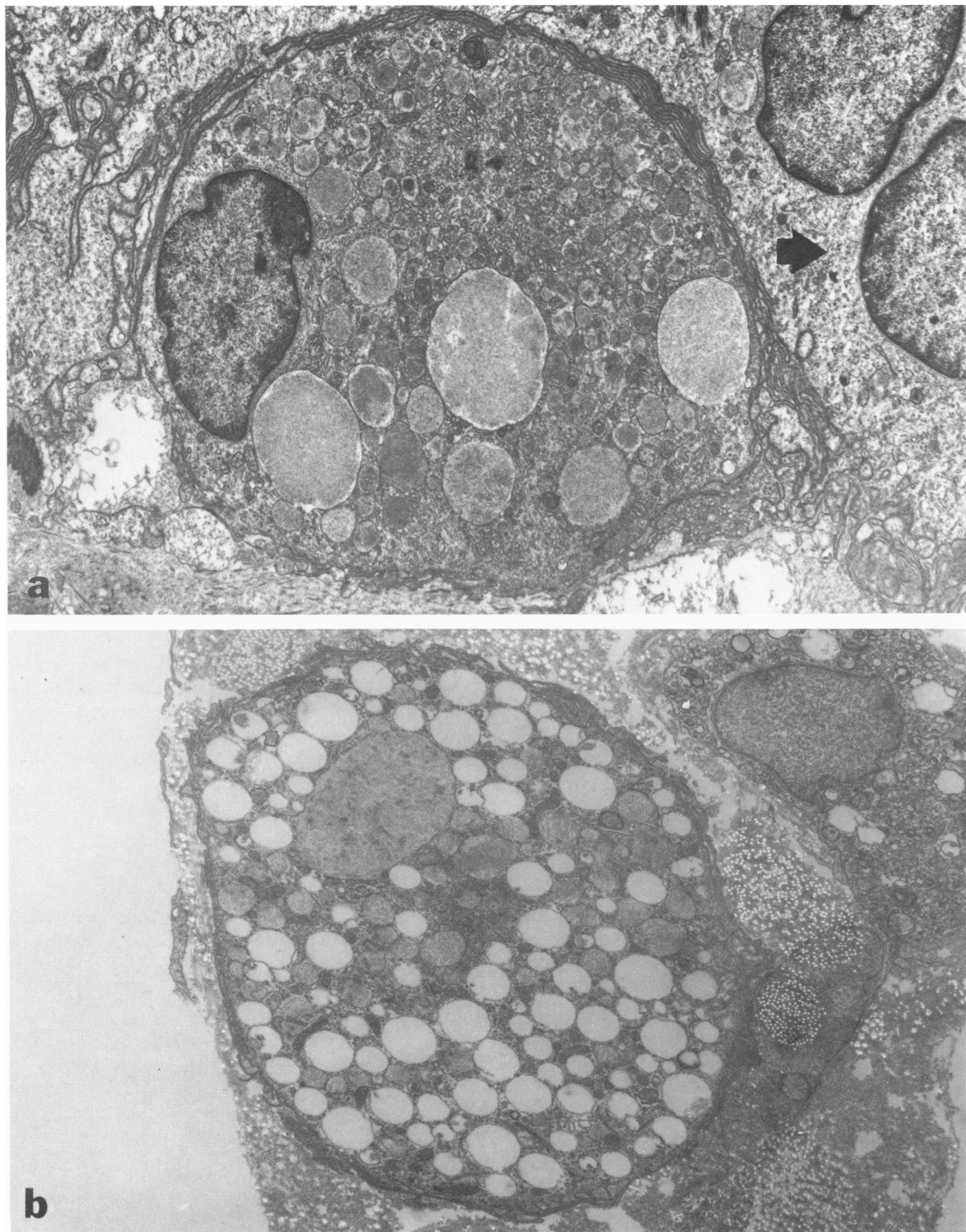


**Figure 5a** – NC 28-day macrophage with large and small lysosomal inclusions. A portion of a polykaryon (*arrow*) is seen to the right. Complex multilamellar membranous arrays partially surround the cell. ( $\times 4500$ ) **b** – HC 28-day foam cell with multiple small electron-translucent, mostly membrane-bound inclusions and both large and small carrageenan-containing inclusions. Collagen is present extracellularly. ( $\times 6100$ )

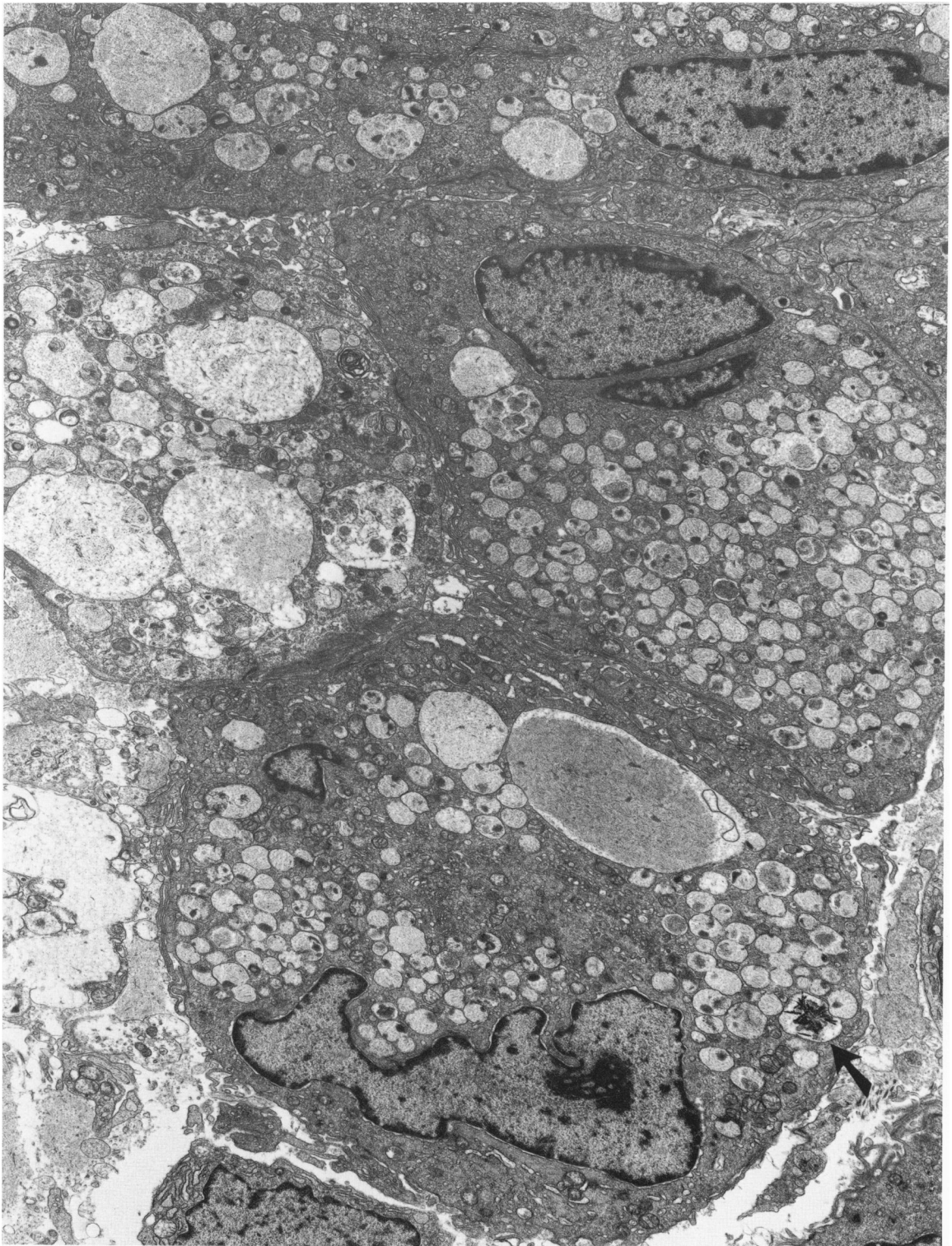


**Figure 6** — NC 28-day granuloma macrophages in close apposition with complex interdigitating processes. Large and small floccular or reticular inclusions, some showing fusion, are prominent. There is a crystalline structure, probably calcific, within a membrane-bound inclusion (arrow). ( $\times 5500$ )



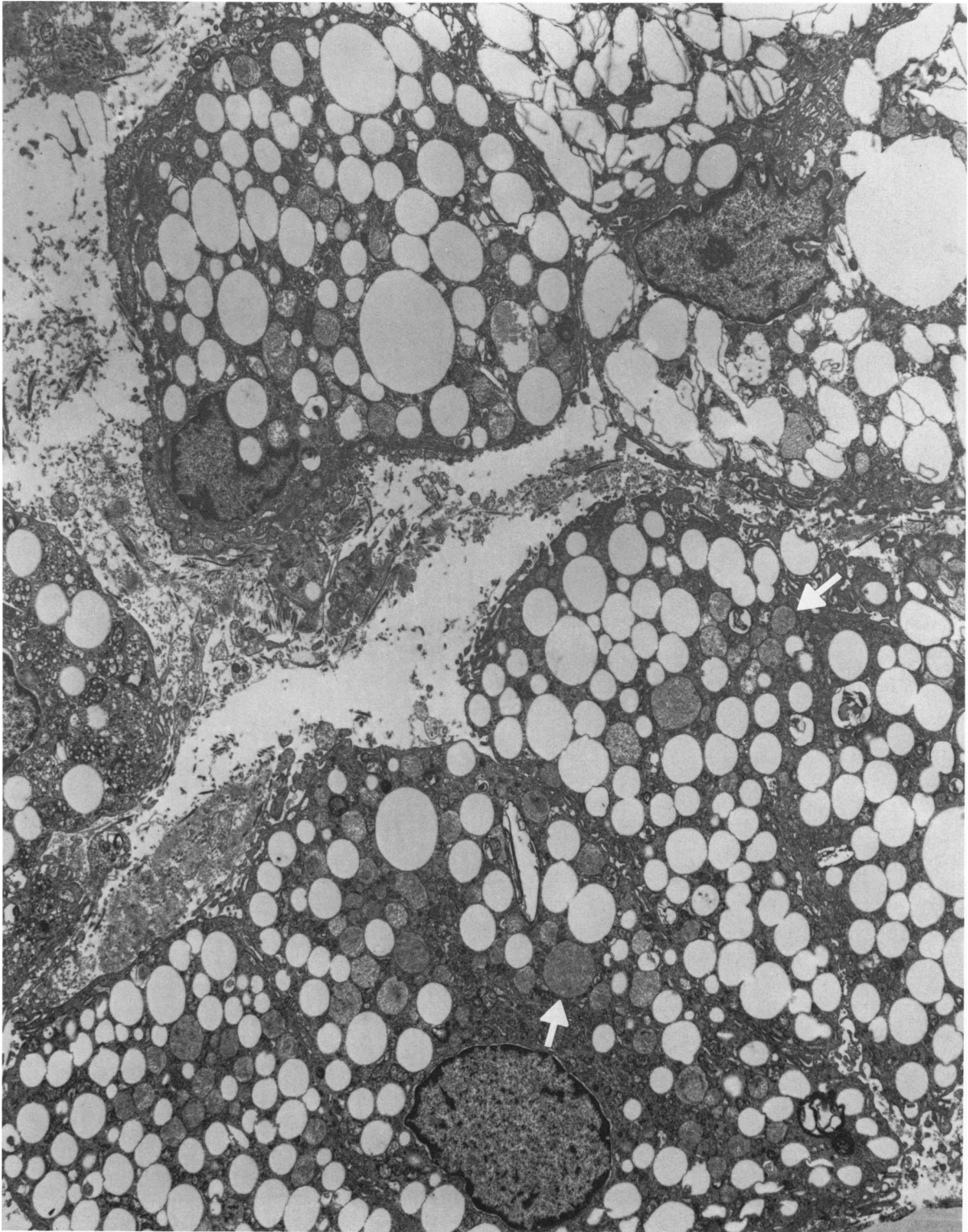


**Figure 7** — HC 28-day granuloma showing several ovoid or polyhedral foam cells in close apposition, and distended by large numbers of electron-translucent inclusions, some exhibiting fusion. Smaller numbers of putative carrageenan-containing inclusions (*arrow*) are present. Nuclear heterochromatin shows peripheral condensation. ( $\times 7500$ )



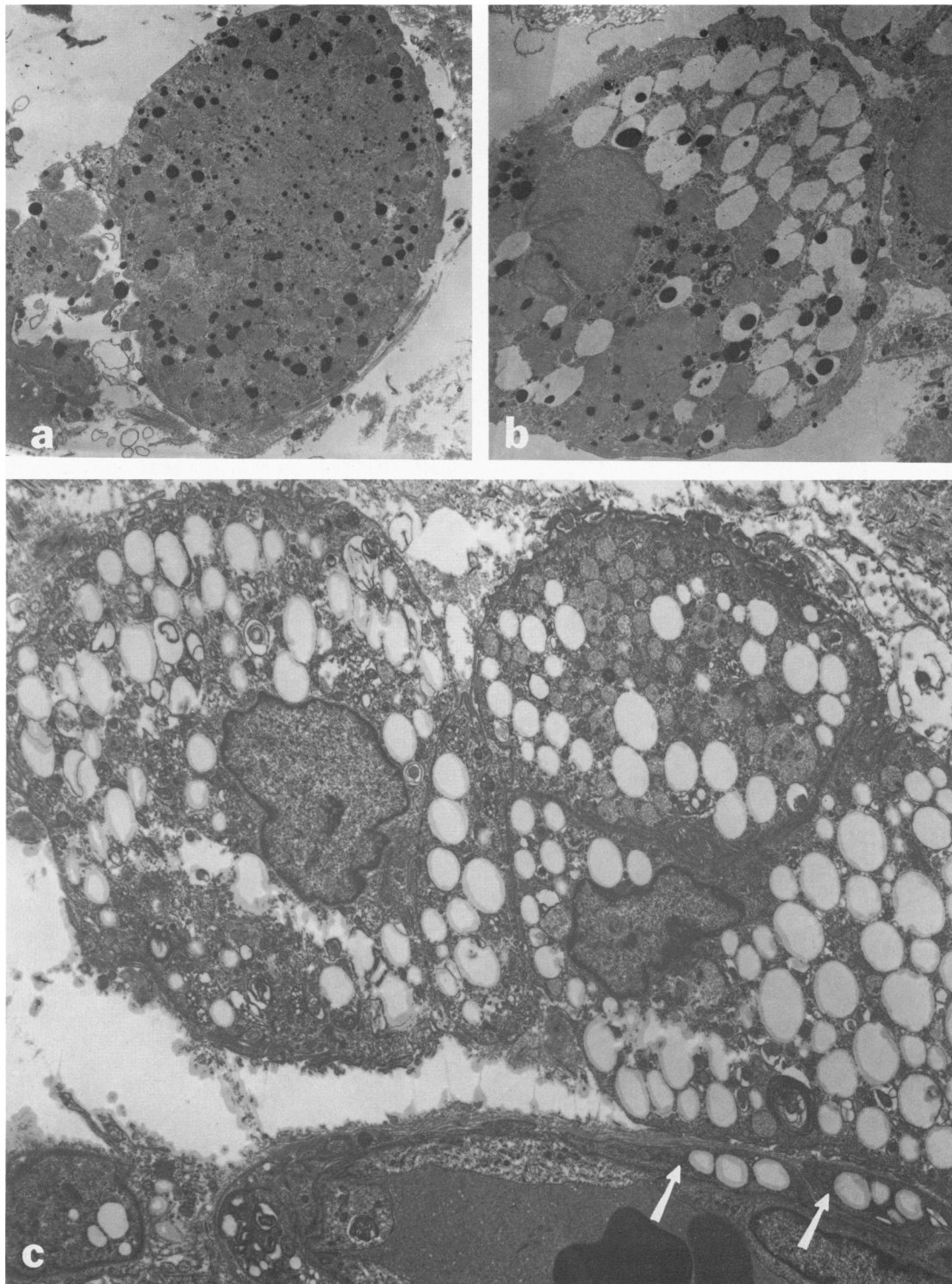


**Figure 8a** – NC 28-day macrophage showing NSE reaction product both within inclusions and in the cytoplasm. ( $\times 5700$ ) **b** – HC 28-day foam cell showing NSE reaction product within electron-translucent inclusions and in the cytoplasm. ( $\times 4800$ ) **c** – HC 28-day granuloma showing portions of 4 foam cells. Electron-translucent inclusions, mostly small, are prominent; some have no distinct limiting membranes, and others appear to be coalescing. Myelin forms are frequent. Two vascular smooth-muscle cells (*arrows*) contain several lipid inclusions and small crystalline structures. ( $\times 10,100$ )

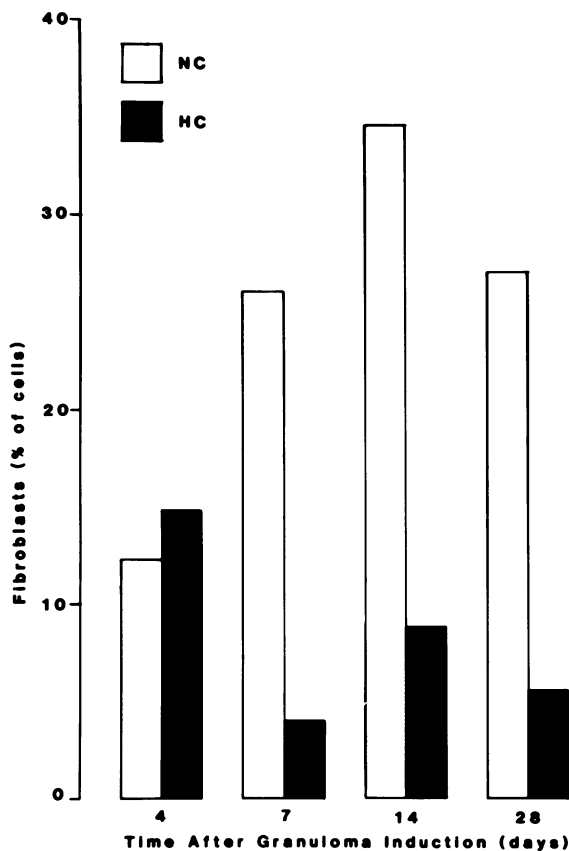


**Figure 9**—The relative distribution of fibroblastlike cells in NC and HC granulomas expressed as a percentage of the total number of cells identified ultrastructurally, within each time and diet group.

leads to the development of chronic granulomatous inflammation in the guinea pig, the carrageenan model has been extensively employed in both skin and lung in the study of the composition, evolution, and cellular kinetics of chronic granulomatous inflammation in a number of species.<sup>36-42</sup> In the present study, the temporal evolution of the carrageenan granuloma in the normocholesterolemic (NC) rabbit was found to be similar to that observed in mice, rats, and guinea pigs.<sup>36,37,40</sup> Although small numbers of granulocytes were seen at 4, 7, and 14 days, it is likely that they were present in greater numbers within the first 24-48 hours,<sup>36,37</sup> and that by 4 days, the acute inflammatory response to carrageenan had largely subsided. From 4-28 days the predominant cells were large macrophages, with lysosomal floccular carrageenan inclusions, accounting for some 80-90% of the cells identified (Table 1). These cells, with prominent cytoplasmic projections, indented or reniform nuclei, and peripheral condensation of nuclear heterochromatin, were NSE-positive at both the light-microscopic and ultrastructural levels, consistent with their origin from

blood monocytes. Monocytes of characteristic morphology were most frequent in the 4-day granulomas (Table 1) and were inconspicuous thereafter, suggesting that a continuing blood monocyte recruitment to the evolving granulomas does not contribute significantly to their later evolution and cellular composition. This conclusion is consistent with the characterization of the carrageenan granuloma as a low-turnover lesion, in which the constituent macrophages have a long life of 2 months or more and are augmented by a low rate of fresh monocyte recruitment and cell division.<sup>38,40</sup> Ryan and Spector<sup>38</sup> found that in 1-week-old granulomas, macrophage nuclear labeling with <sup>3</sup>H-thymidine averaged 2%, while at 2 and 4 weeks, the percentage of macrophages exhibiting DNA synthesis was less than 1% and 0.3%, respectively. Such low rates of cell division are in agreement with the low frequency of macrophage mitoses observed in this study.

It is noteworthy that the macrophages in the NC granulomas exhibited little or no ORO-stainable neutral lipid at any of the time points studied (Figure 2c), and that cytoplasmic lipid inclusions were inconspicuous (Figures 3a, 4a, 5a, and 6). These morphologic findings are consistent with the lipid composition of 3- and 8-day guinea pig carrageenan granulomas.<sup>43</sup> Levin and Head<sup>43</sup> found relatively low levels of monoglycerides, diglycerides, sterols, and sterol esters, the principal component being triglycerides, a finding we consider probably represents contaminating adipose tissue. Our own compositional data<sup>27</sup> have confirmed the paucity of neutral lipid classes both in evolving NC rabbit carrageenan granuloma tissue and in macrophages isolated and cultured from the granulomas.

Additional morphologic features of the NC granulomas deserve brief comment. Fibroblasts, often with



**Figure 10**—Scanning electron micrograph of a 24-hour culture on glass derived from an HC 14-day granuloma. The macrophages show extensive attachment aprons and elongate cytoplasmic processes. ( $\times 1150$ )

a prominent and dilated RER, were observed at all times studied and were almost three times more frequent at 14 days, relative to the 4-day lesions (Figure 9). This increasing fibroblast proliferation may reflect the macrophage secretion of a mitogen, or macrophage-derived growth factor (MDGF), which has been shown to stimulate the growth of fibroblasts, vascular smooth-muscle cells, and endothelial cells in culture.<sup>44</sup> Similarly, the vascularization of the granuloma may, at least in part, result from macrophage-induced capillary proliferation.<sup>45-47</sup>

Lymphocytes and plasma cells were present sporadically and in small numbers in evolving granulomas, in all likelihood reflecting a relatively low-level cellular immunologic response to the carrageenan. Large epithelioid cells were frequent, often showing complex multilaminar interdigitating arrays of their plasmalemmal membranes, particularly when in apposition. Polykaryons were likewise frequent and appeared to originate by fusion of the epithelioid cells.<sup>48</sup> The ultimate biologic role(s) of both the epithelioid cell and the polykaryon in the evolving carrageenan granuloma and the stimuli for their differentiation remain uncertain. It is feasible, however, that the multinucleate giant cell may have a function analogous to that of the osteoclast in calcium mobilization and calcification.<sup>49</sup>

Cholesterol-oil dietary supplementation resulted in moderate levels of hypercholesterolemia and an associated dyslipoproteinemia in which the principal lipoprotein class was cholesteryl-ester-rich very-low-density lipoprotein (VLDL).<sup>27</sup> This dietary manipulation had a profound effect on the morphology of the evolving granulomas, and in the 28-day lesions 69% of the cells had assumed the characteristic morphology of foam cells, their cytoplasm distended by large numbers of electron-translucent lipid inclusions (Figures 4b, 5b, 7, and 8c). It is important to note that a transitional spectrum from the early carrageenan-containing macrophage to the fully developed foam cell was observed (Figure 4b); and, further, in the 28-day lesions, where foam cells were most numerous, there was a proportionate decline in the number of macrophages. These findings indicate that granuloma macrophages exposed to high levels of plasma cholesterol exhibit a serial differentiation into foam cells *in situ*, and that any foam-cell recruitment from the circulation as has been implicated for the artery wall in atherogenesis<sup>50,51</sup> is unlikely to augment the granuloma foam-cell population significantly, although some such contribution cannot be excluded.

HC granuloma macrophages were distinguishable from their NC counterparts as early as 4 days. In particular, they exhibited striking ORO-positive neutral lipid accumulation (Figure 2d), which was reflected

ultrastructurally by the presence of variable numbers of small electron-translucent mostly membrane-bound lipid inclusions. Additionally, the HC macrophages showed a distinct excess of myelin bodies, both within lysosomes and in the cytoplasm (Figures 4b and 8c). This phenomenon persisted through 7, 14, and 28 days, and presumably in part accounts for the phospholipid content of the HC macrophages and foam cells observed.<sup>27</sup> With an increasing duration of exposure to high plasma cholesterol, the numbers of small cytoplasmic lipid inclusions increased, and their morphology changed somewhat. In particular, from 7 days and onward, an increasing coalescence or fusion of the inclusions was observed (Figure 7); and, further, inclusions with incomplete or absent limiting membranes became more frequent. These observations may indicate that macrophage lysosomal membranes become increasingly fragile during cellular lipid accumulation. However, it is possible that some non-membrane-bound cytoplasmic lipid inclusions have arisen *de novo*, rather than through disruption of lysosomal membranes. Both cytoplasmic lipid droplets and lysosomal membrane-bound lipid inclusions occur within rabbit arterial foam cells, and both are sites for cholesteryl ester accumulation.<sup>52,53</sup>

Maltese crosses, indicating the presence of cholesteryl esters, were seen within cultured HC macrophages and foam cells under polarized light, consistent with the markedly elevated cholesteryl ester content of both the HC granuloma tissue and macrophages/foam cells cultured from HC granulomas.<sup>27</sup> It is of interest also that acicular crystalline structures, probably representing crystalline unesterified cholesterol, were occasionally observed ultrastructurally in some of the foam cells.

While the lipid composition of evolving granuloma foam cells and the pathways involved in their lipid accumulation are described and discussed in a companion study,<sup>27</sup> some brief comments are appropriate at this time. It has been shown that hypertriglyceridemic VLDL induces both triglyceride synthesis and accumulation in resident mouse peritoneal macrophages<sup>54</sup> but does not enhance the incorporation of oleate into cholesteryl esters. On the other hand, malondialdehyde-altered LDL (MDA-LDL), which enters the monocyte-macrophage via a receptor for negatively charged proteins (scavenger receptor pathway), leads to significant cholesteryl ester accumulation.<sup>55</sup> A similar phenomenon has been demonstrated with both acetyl-LDL<sup>56,57</sup> and  $\beta$ -VLDL,<sup>58</sup> which lead to both cholesteryl ester accumulation in macrophages<sup>56-58</sup> and an increased rate of cholesteryl ester synthesis from <sup>14</sup>C-oleate.<sup>54,56-58</sup> The cholesteryl ester accumulation in HC granuloma macrophages and foam cells observed in the present study in response to elevated plasma lipoprotein levels<sup>27</sup> ap-

pears analogous to the response of macrophages to either altered LDL (MDA-LDL, acetyl-LDL) or a naturally occurring lipoprotein,  $\beta$ -VLDL. At present, we are unable to comment on how the presence of ingested carrageenan may influence this response or how the secretory products of the granuloma macrophages released into the extravascular space may modify lipoproteins and their subsequent internalization and catabolism. In the latter context, it has been shown that LDL appears to be modified in interstitial inflammatory fluid.<sup>59</sup>

This study has established that monocyte-macrophages, recruited subcutaneously in response to carrageenan and exposed to high plasma cholesterol levels *in vivo*, are able to differentiate into foam cells typical of those encountered in atheroma. The model should prove useful for the further characterization of mechanisms involved in cellular cholesterol ester accumulation.

### References

- Schwartz CJ, Mitchell JRA: Cellular infiltration of the human arterial adventitia associated with atheromatous plaques. *Circulation* 1962, 26:73-78
- Schwartz CJ, Mitchell JRA: The morphology, terminology and pathogenesis of arterial plaques. *Postgrad Med J* 1962, 38:25-34
- Mitchell JRA, Schwartz CJ: *Arterial Disease*. Oxford, Blackwell Scientific Publications, 1965, p 30
- Duff GL, McMillan GC, Ritchie AC: The morphology of early atherosclerotic lesions of the aorta demonstrated by the surface technique in rabbits fed cholesterol. *Am J Pathol* 1957, 33:845-873
- Barbolini G, Scilabra GA, Botticelli A, Botticelli S: On the origin of foam cells in cholesterol-induced atherosclerosis of the rabbit. *Virchows Arch [Cell Pathol]* 1969, 3:24-32
- Schaffner T, Taylor K, Bartucci EJ, Fischer-Dzoga K, Besson JH, Glagov S, Wissler RW: Arterial foam cells with distinctive immunomorphologic and histochemical features of macrophages. *Am J Pathol* 1980, 100:57-80
- Still WJS, O'Neal RM: Electron microscopic study of experimental atherosclerosis in the rat. *Am J Pathol* 1962, 40:21-35
- Joris I, Zand T, Nunnari JJ, Krolikowski FJ, Majno G: Studies on the pathogenesis of atherosclerosis: I. Adhesion and emigration of mononuclear cells in the aorta of hypercholesterolemic rats. *Am J Pathol* 1983, 113:341-358
- Gerrity RG, Naito HK, Richardson M, Schwartz CJ: Dietary induced atherogenesis in swine. *Am J Pathol* 1979, 95:775-792
- Gerrity RG, Schwartz CJ: Endothelial cell injury in early mild hypercholesterolemia. *Prog Biochem Pharmacol* 1977, 13:213-219
- Gerrity RG: The role of the monocyte in atherogenesis: I. Transition of blood-borne monocytes into foam cells in fatty lesions. *Am J Pathol* 1981, 103:181-190
- Lewis JC, Taylor RG, Jones ND, StClair RW, Cornhill JF: Endothelial surface characteristics in pigeon coronary artery atherosclerosis: I. Cellular alterations during the initial stages of dietary cholesterol challenge. *Lab Invest* 1982, 46:123-138
- Schwartz CJ, Fine R, Kelley JL, Sprague EA, Jauchem JR: Monocyte recruitment in the normal and atheromatous nonhuman primate aorta. *Circulation* 1980, 62(Suppl III):96
- Stary HC: The intimal macrophage in atherosclerosis. *Artery* 1980, 8:205-207
- Kelley JL, Sprague EA, Carey KD, Valente AJ, Suenram CA, Schwartz CJ: Atherosclerosis in vervet monkeys (*Cercopithecus aethiops*) after a 7-year dietary challenge. (Manuscript in preparation)
- Van Furth R: Origin and kinetics of monocytes and macrophages. *Semin Hematol* 1970, 7:125-141
- Stossel TP: Phagocytosis. *N Engl J Med* 1974, 290:717-723, 774-780, 833-839
- Unanue ER: Secretory function of mononuclear phagocytes: A review. *Am J Pathol* 1976, 83:396-417
- Unanue ER: The macrophage as a regulator of lymphocyte function. *Hosp Practice* 1979, Nov:61-74
- Pierce CW: Macrophages: Modulators of immunity. *Am J Pathol* 1980, 98:10-28
- Schwartz CJ, Sprague EA, Fowler SR, Kendall JI, Kelley JL, Valente AJ: Evolution of lipid-rich macrophages in experimental granulomas. *Circulation* 1982, 66(II):225
- Allain CC, Poon LS, Chan CSG, Richmond W, Fu PC: Enzymatic determination of total serum cholesterol. *Clin Chem* 1974, 20:470-475
- Yam LT, Li CY, Crosby WH: Cytochemical identification of monocytes and granulocytes. *Am J Clin Pathol* 1971, 55:283-290
- Li CY, Yam LT, Crosby WH: Histochemical characterization of cellular and structural elements of the human spleen. *J Histochem Cytochem* 1972, 20:1049-1058
- Kim H, Pangalis GA, Payne BC, Kadin ME, Rappaport H: Ultrastructural identification of neoplastic histiocytes-monocytes: An application of a newly developed cytochemical technique. *Am J Pathol* 1982, 106:204-223
- Sprague EA, Kelley JL, Schwartz CJ: Growth, structure and function of baboon aortic smooth muscle cells in culture. *Exp Molec Pathol* 1982, 37:48-66
- Kelley JL, Suenram CA, Valente AJ, Sprague EA, Schwartz CJ: Evolution of foam cells in subcutaneous rabbit carrageenan granulomata: II. Tissue and macrophage lipid composition. (Manuscript submitted)
- Smith DB, Cook WH: Fractionation of carrageenan. *Arch Biochem Biophys* 1953, 45:232-233
- DiRosa M: Biological properties of carrageenan. *J Pharm Pharmacol* 1972, 24:89-102
- O'Neill AN: 3,6-Anhydro-D-galactose as a constituent of  $\alpha$ -carrageenin. *J Am Chem Soc* 1955, 77:2837-2839
- O'Neill AN: Derivatives of 4-O- $\beta$ -D-galactopyranosyl-3,6-anhydro-D-galactose from  $\alpha$ -carrageenin. *J Am Chem Soc* 1955, 77:6324-6326
- Smith DB, O'Neill AN, Perlin AS: The heterogeneity of carrageenin. *Canad J Chem* 1955, 33:1352-1360
- Atkinson RM, Jenkins L, Tomich EG, Woollett EA: The effects of some antiinflammatory substances on carrageenin-induced granulomata. *J Endocrinol* 1962, 25:87-93
- McCandless EL: Chemical structural requirements for stimulation of connective tissue growth by polysaccharides. *Ann New York Acad Sci* 1965, 118:869-881
- Robertson W van B, Schwartz B: Ascorbic acid and the formation of collagen. *J Biol Chem* 1953, 201:689-695
- Williams G: A histological study of the connective tissue reaction to carrageenin. *J Pathol Bacteriol* 1957, 73:557-563
- Monis B, Weinberg T, Spector GJ: The carrageenan granuloma in the rat: A model for the study of the structure and function of macrophages. *Br Exp Pathol* 1968, 49:302-310
- Ryan GB, Spector WG: Natural selection of long-lived



- macrophages in experimental granulomata. *J Pathol* 1969, 99:139-151
39. Pérez-Tamayo R: Collagen resorption in carrageenin granulomas: I. Collagenolytic activity in *in vitro* explants. *Lab Invest* 1970, 22:137-141
  40. Papadimitriou JM, Spector WG: The ultrastructure of high- and low-turnover inflammatory granulomata. *J Pathol* 1972, 106:37-43
  41. Arenal P, Pérez-Tamayo R: The nature of collagen in the carrageenin granuloma. *Proc Soc Exp Biol Med* 1973, 142:1031-1035
  42. Bowers RR, Stapleton ME, Lew PD: An ultrastructural study of the macrophages of the carrageenan-induced granuloma in the rat lung. *J Pathol* 1983, 140:29-40
  43. Levin E, Head C: Lipids of connective tissue: I. The *in vitro* incorporation of acetate- $^{14}C$  into neutral lipids of the carrageenin granuloma. *J Lab Clin Med* 1965, 66:750-757
  44. Martin BM, Gimbrone MA, Unanue ER, Cotran RS: Stimulation of nonlymphoid mesenchymal cell proliferation by a macrophage-derived growth factor. *J Immunol* 1981, 126:1510-1515
  45. Poverini PJ, Cotran RS, Sholley MM: Endothelial proliferation in the delayed hypersensitivity reaction: An autoradiographic study. *J Immunol* 1977, 118:529-532
  46. Greenburg GB, Hunt TK: The proliferative response *in vitro* of vascular endothelial and smooth muscle cells exposed to wound fluids and macrophages. *J Cell Physiol* 1978, 97:353-360
  47. Thakral KK, Goodson WH III, Hunt TK: Stimulation of wound blood vessel growth by wound macrophages. *J Surg Res* 1979, 26:430-436
  48. Sutton JS, Weiss L: Transformation of monocytes in tissue culture into macrophages, epithelioid cells, and multinucleated giant cells: An electron microscopic study. *J Cell Biol* 1966, 28:303-332
  49. Kahn AJ, Stewart CC, Teitelbaum SL: Contact-mediated bone resorption by human monocytes *in vitro*. *Science* 1978, 199:988-990
  50. Simon RC, Still WJS, O'Neal RM: The circulating lipophage and experimental atherosclerosis. *J Atheroscler Res* 1961, 1:395-400
  51. Suzuki M, O'Neal RM: Circulating lipophages, serum lipids, and atherosclerosis in rats. *Arch Pathol* 1967, 83:169-174
  52. Shio H, Haley NJ, Fowler S: Characterization of lipid-laden aortic cells from cholesterol-fed rabbits: II. Morphometric analysis of lipid-filled lysosomes and lipid droplets in aortic cell populations. *Lab Invest* 1978, 39:390-397
  53. Shio H, Haley NJ, Fowler S: Characterization of lipid-laden aortic cells from cholesterol-fed rabbits: III. Intracellular localization of cholesterol and cholesteryl ester. *Lab Invest* 1979, 41:160-167
  54. Gianturco SH, Bradley WA, Gotto AM, Morrisett JD, Peavey DL: Hypertriglyceridemic very low density lipoproteins induce triglyceride synthesis and accumulation in mouse peritoneal macrophages. *J Clin Invest* 1982, 70:168-178
  55. Fogelman AM, Shechter I, Seager J, Hokom M, Child JS, Edwards PA: Malondialdehyde alteration of low density lipoproteins leads to cholesteryl ester accumulation in human monocyte-macrophages. *Proc Natl Acad Sci* 1980, 77:2214-2218
  56. Brown MS, Goldstein JL, Krieger M, Ho YK, Anderson RGW: Reversible accumulation of cholesteryl esters in macrophages incubated with acetylated lipoproteins. *J Cell Biol* 1979, 82:597-613
  57. Albert DH, Traber MG, Kayden HJ: Cholesterol metabolism in human monocyte-derived macrophages: Stimulation of cholesteryl ester formation and cholesterol excretion by serum lipoproteins. *Lipids* 1982, 17:709-715
  58. Mahley RW, Innerarity TL, Brown MS, Ho YK, Goldstein JL: Cholesteryl ester synthesis in macrophages: Stimulation by  $\beta$ -very low density lipoproteins from cholesterol-fed animals of several species. *J Lipid Res* 1980, 21:970-980
  59. Raymond TL, Reynold SA: Lipoproteins of the extravascular space: Alterations in low density lipoproteins of interstitial inflammatory fluid. *J Lipid Res* 1983, 24:113-119

### Acknowledgments

We thank Mrs. P. Pegg and Ms. A. Garcia for secretarial help. S. Fowler, PhD, postdoctoral fellow in the Department of Pathology, participated in the early phases of this study. The technical assistance of D. Guerrero, C. Levy, and F. Elias with the ultrastructural aspects of this study is much appreciated.